International Journal of Engineering Innovation & Research
Volume 1, Issue 5, ISSN : 2277 – 5668

Simultaneous Detection of Radial Deformation Location and Axial Displacement Extent in a Transformer Winding Using Cross-correlation Technique and ANN

M. Rahmatian matin.rahmatian@aut.ac.ir
M. S. Naderi salaynaderi@aut.ac.ir
G. B. Gharehpetian grptian@aut.ac.ir
A. J. Ghanizadeh ghanizadeh@aut.ac.ir

***Abstract* — In this paper, a new method to detect and locate mechanical defects, as one of the major faults in power transformer windings, is proposed. Axial displacement and radial deformation are considered as two major types of mechanical defects in this study. In the first step, a real transformer winding is modelled based on detailed model considering geometrical specifications and the frequency response characteristics are obtained for intact and defected modes. This technique is called Frequency Response Analysis (FRA). Thereafter, some features based on cross-correlation and other mathematical patterns are selected from the obtained signals. These features are then used to train an ANN classifier. The proposed method is able to discriminate between radial deformation and axial displacement defects precisely and determine the axial displacement extent and radial deformation location with a good accuracy. This accuracy rate reaches 81.25% for axial displacement extent and 75% for radial deformation location.**

***Keywords* — Radial Deformation (RD), Axial Displacement (AD), Feature selection, Artificial Neural Network (ANN).**

I. INTRODUCTION

Transformer windings may be exposed to severe electromechanical forces following short circuit currents. Although these forces may not lead to an immediate failure of a transformer, they can make the transformer more vulnerable in such situations. Electromechanical forces can damage the transformer in two main forms, i.e., Radial Deformation (RD) and Axial Displacement (AD). Consequently, researches should be concentrated on detection of these two defect types to inform the operators and prevent transformers from a sudden failure.

A powerful tool for detection of mechanical defects is Frequency Response Analysis (FRA) [1]. FRA depends on geometrical characteristics of the winding and mechanical changes in the winding structure can affect it at different frequency intervals [2, 3]. Hence, the comparison between the FRA of an operating transformer with its original one can lead to detection of mechanical defects. Four main comparison algorithms for FRA are introduced in the literature based on artificial methods, exact calculations, estimation methods and electric circuit models [4].

Besides experimental tests, it is possible to obtain the FRA from an appropriate transformer model. Detailed model is a suitable model validated for the range of 10 kHz < f < 1 MHz and can represent mechanical defects [5]. This model is comprised of different resistances, capacitances and inductances and mechanical defects change these parameters.

A method for determining the level and location of mechanical defects is presented in [6]. However, it is only possible to determine in which section among the winding three sections, i.e., earth end, mid section, and line section, the fault is located. In [4], mechanical defects are detected and located using some mathematical features, but different windings are investigated for AD and RD.

In this paper, a real transformer winding is modeled based on detailed model considering its geometrical characteristics. Thereafter, the parameters of the detailed model are calculated following different mechanical defects and the frequency responses are obtained for each case. In the next step, different features are applied to the obtained signals and the obtained features are used to train an ANN as the regression method. Through this new method it is possible to detect the type, extent and location of mechanical defects in transformer windings.

II. DETAILED MODEL

Through detailed model, a comprehensive and precise analysis of transformer windings behaviour and their mutual interactions is possible. In the detailed model applied in this paper, each double-disc is assumed as the smallest equipotentional unit and modelled by a predetermined set of electrical lumped elements.

Fig.1 shows the schematic of the transformer winding under study. The HV winding is constructed of 30 double-discs with 11 rings on each disc while the LV winding is a two-layered one, composed of six parallel conductors. The voltage and power transfer rate of the transformer are 10 kV/ 400 V and 1.2 MVA, respectively.

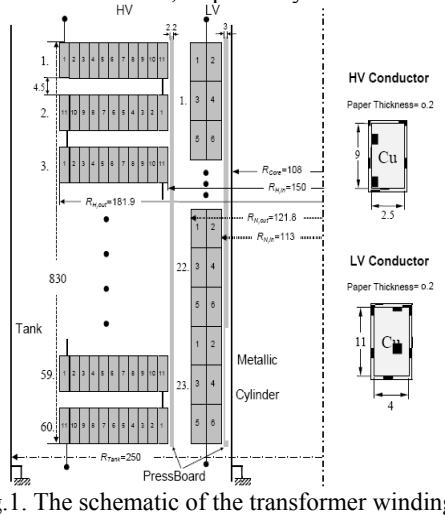

Fig.1. The schematic of the transformer windings

Fig. 2 shows the circuit diagram for detailed model where C_e, R_e, C_{HL}, L, M, K show the earth capacitance,

insulation resistance, the capacitance between LV and HV windings, self and mutual inductances and parallel capacitance of each double-disc, respectively.

For an accurate simulation of the winding frequency behavior, the parameters of the detailed model should be calculated, precisely. In the following subsections, the analytical formulas for calculation of the model elements are presented.

A. Self and Mutual Inductances

The third and forth Maxwell's equations are applied to calculate the self and mutual inductances in this model. These equations can be stated as follows [7]:

$$M_{12} = \frac{\mu_0}{4\pi} \oint_{C_1} \oint_{C_2} \frac{d\vec{s}_1 . d\vec{s}_2}{R_{12}} \tag{1}$$

This integral can be stated more specifically as follows:

$$M_{12} = \frac{\mu_0}{4\pi} \int_0^{2\pi} \int_0^{2\pi} \frac{r_1(\alpha_1).r_2(\alpha_2).cos(\alpha_2 - \alpha_1)}{R_{12}(\alpha_1, \alpha_2)} .d\alpha_1 .d\alpha_2 \tag{2}$$

Using the numeric trapezoidal rule, the above integral can be calculated through the following closed formula [8]:

$$M_{12} = \frac{2\mu_0 \sqrt{r_1 r_2}}{\sqrt{k'}} .\left[K(k') - E(k')\right] \tag{3}$$

where *E(k')* and *K(k')* are the first and second type of the complete Elliptical integrals and *k'* is obtained as follows:

$$k' = \frac{1-\sqrt{1-k^2}}{1+\sqrt{1+k^2}}, \tag{4}$$

$$k = \sqrt{\frac{4r_1 r_2}{(r_1 + r_2)^2 + d^2}} \tag{5}$$

The mutual inductance between two different discs can be obtained by summing the mutuality between the turns of them. This relation can be applied to calculate the self inductance, too.

B. Capacitances

In Fig. 2, it can be seen that different capacitances, i.e., K_i, C_{HL} and C_e are embedded in the circuit. K_i is a representative for the electric field between two consecutive discs along the winding. Similarly, C_{HL} and C_e are the models of the electric fields between the high and low windings and between the windings and the tank, respectively.

Theses capacitances can be calculated based on a homogenous or a cylindrical distribution of the electrical field. It should be noted that the appropriate correction factors are needed for considering the edge effects when using homogenous formulas. In this paper, the homogenous relations are applied [9, 10].

C. Resistances

Since the detailed model is applied for high frequency analysis (f > 10 kHz), the magnetic field penetration in the core is low and there is no need to the model the core loss. Resistances in the detailed model are applied to model the losses of the winding (R_{si}) and the insulation or dielectric loss (R_p or R_e). R_{si} includes copper losses in addition to proximity and skin effect [11].

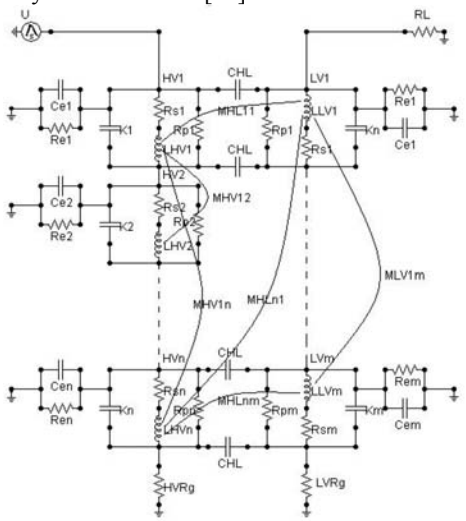

Fig.2. Detailed model of the transformer winding

III. MECHANICAL DEFECTS

In this section two types of mechanical defects are under study, i.e., RD and AD. These two types of mechanical defects are the most common ones in transformer windings while other mechanical defects may rarely occur such as disc space variation or hybrid forms.

RD (forced buckling mode) leads to changes in the electric and magnetic fields of the winding. The winding discs can be deformed in 1-side up to 4-side. Fig. 3 illustrates these different deformation degrees.

It is proved that RD mainly affects the capacitances in the detailed model [12]. Since the deformation occurs in the output layer of HV winding, this deformation results in decrease of the capacitance between the output layer and the transformer tank.

Considering Fig. 3, the radius in RD defect is modelled as below:

$$r(\theta) = \begin{cases} r_0 + \dfrac{d}{2}(\cos(s\theta) - 1) & for \quad 0 \le \theta \le \dfrac{2\pi}{s} \\ otherwise\ r_0 \end{cases} \tag{6}$$

where r_0 is the radius of the winding in non-deformed mode, d is the deformation depth, s is the deformation span width and θ is the angle.

In this mode, the capacitance between the HV winding and the transformer tank can be calculated as follows:

$$C_i = \sum_{\theta=0}^{2\pi} \left(\frac{2\pi\varepsilon_0\varepsilon_r}{\ln r_0 / r(\theta)}\right).\Delta\theta \tag{7}$$

where ε_r and ε_0 are dielectric constant and permittivity, respectively and $\Delta\theta$ is the segment of angle.

AD defect leads to changes in the height of the windings with respect each other. In contrast to the RD, AD predominantly results in changes in mutual inductances and the changes in capacitances can be ignored [12]. As a result of variations in the windings height, the vertical distance between different discs and mutual inductances

change. In this mode, again (3) is applied to calculate the mutual inductances.

IV. Data Acquisition

Different terminal connections can be considered for transformer winding investigations [12]. In this paper, a schematic shown in Fig. 4 is under investigation. Therefore, the HV winding is grounded and the LV winding terminals are open. The detailed model results are validated up to 1 MHz in the frequency range.

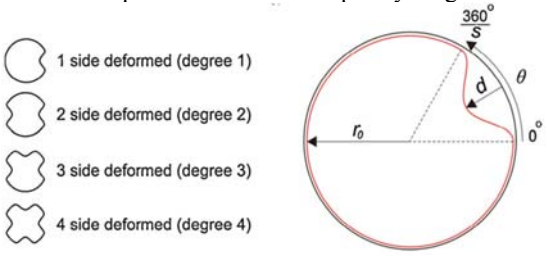

Fig.3. Different degrees of radial deformation of HV winding

Therefore, the transformer winding is swept in this range. Each signal consists of 10000 samples in the span of 0-1MHz.

For RD, each consecutive 6 discs are deformed for four degrees and hence, 4x10 signals are obtained and saved for all the length of the HV winding. The depth of deformation is equal to 12% of the HV winding radius and the span of deformation is 45°. Fig. 5 shows the results of the FRA simulation at different RD locations for 4-side deformation.

Similarly, in AD, to consider the upward and downward movements of the winding, first the HV winding is lowered until its bottom is completely located lower than the bottom of the LV winding. Thereafter, the HV winding is displaced upwardly equal to 0.5 cm in each step and frequency response is obtained again. The total displacement is equal to 10% of the whole winding height. In this part, 16 test signals are obtained and saved. Fig. 6 shows the admittance transfer function for different HV winding displacements.

V. Proposed Schemes

The scheme proposed here, is composed of two stages, i.e., feature selection and ANN for classification. Each stage is described in the next sub-sections.

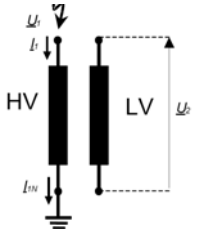

Fig.4. The schematic of terminal connection studied in this paper

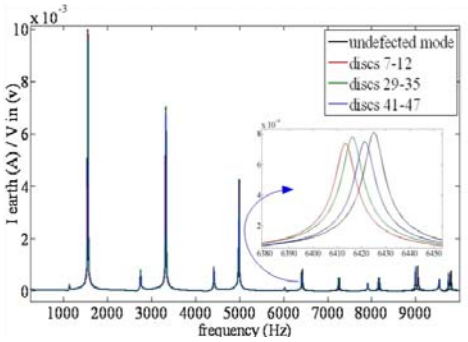

Fig.5. FRA characteristics for different RD cases

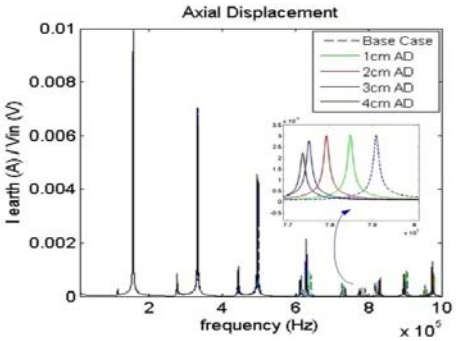

Fig.6. FRA characteristics for different RD cases

A. Feature Selection

In this study, first, the cross-correlation technique is selected as the feature selection method. This technique represents the level of similarity between two signals. In each case, the correlation between the signals obtained from the undefected mode *(A(n))* and the defected mode *(B(n))* is obtained through the relation as follows [13], [14]:

$$\hat{E}_{AB}(m)=\begin{cases}\sum_{n=0}^{W-m-1} A_{n+m}B_n & m\geq 0\\ \hat{E}_{BA}(-m) & m<0\end{cases} \quad (8)$$

where $m= -W, \ldots,-1,0,1,\ldots,+W,$ is time shift parameter, W is the sample number of the signals and subscript AB shows the correlated winding currents. Consequently, the cross-correlation signal consists of $2W+1$ sample numbers. Considering the cross-correlation resultant signal, seven features are selected as follows:

$F1$ = Maximum value of the sequence (E_{max})

$$F2=\frac{\sum_{n=-W}^{W} nE_n}{E_{\max}} \qquad F3=\frac{\sum_{n=-W}^{W} nE_n}{\sum_{n=-W}^{W} E_n}$$

$$F4=\frac{\sum_{n=-W}^{W} |n|E_n}{\sum_{n=-W}^{W} E_n} \qquad F5=\sqrt{\frac{\sum_{n=-W}^{W} n^2E_n}{\sum_{n=-W}^{W} E_n}}$$

$$F6=\sum_{n=-W}^{W}\frac{E_n}{2W+1}$$

$$F7=\sqrt{\frac{\sum_{n=-W}^{W}(E_n-F6)^2}{(2W+1)}}$$

[1] (9)

The second set of features is as follows [15]:

$$ED = \|A(n) - B(n)\| = \sqrt{(A(n) - B(n))^T (A(n) - B(n))} \quad (10)$$

which determines the Euclidean Distance (ED) between signals *A(n)* and *B(n)*,

$$A = \int |\{A(f) - B(f)\} df| \quad (11)$$

which compares the difference in absolute value of the signals area,

$$CC(A,B) = \frac{\sum_{n=1}^{W} A(n)B(n)}{\sqrt{\sum_{n=1}^{W}[A(n)]^2 \sum_{n=1}^{W}[B(n)]^2}} \quad (12)$$

which determines the cross correlation of two signals as an index for calculating the similarity between two signals,

$$SSE(A,B) = \frac{\sum_{n=1}^{W} (A(n) - B(n))^2}{n} \quad (13)$$

which calculates sum squared error and,

$$SSRE(A,B) = \frac{\sum_{n=1}^{W} (\frac{A(n)}{B(n)} - 1)^2}{n} \quad (14)$$

which determines sum squared ratio error.

For instance, two of these features are illustrated in Fig. 7 for AD and two others are illustrated in Fig. 8 for RD. As depicted in these figures, the obtained characteristics for the RD are almost linear while the characteristics for the AD are not injective functions, i.e., for a predetermined amount two heights may be specified. The reason of this behaviour is that during displacing the winding upwardly, some similar situations happen for the winding distances which may result in almost equal values in mutual inductance matrix. If downward displacements are not considered, these features will become linear, too. This disadvantage decreases the accuracy in the axial displacement detection in the classification stage.

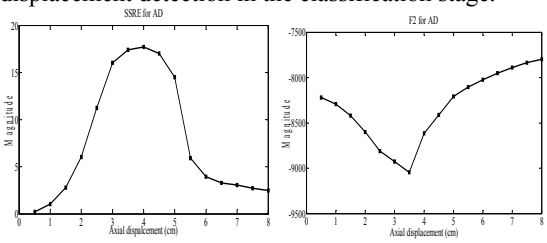

Fig.7.Variations of features SSRE and F2 for axial displacement

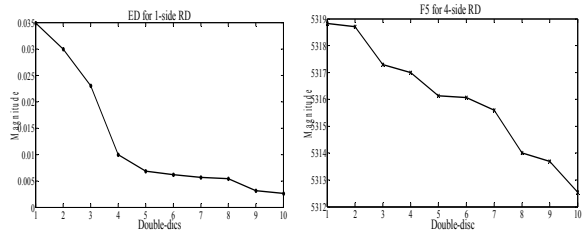

Fig.8. Variations of features ED and F5 for radial deformation

B. Regression Method

Many applications have been considered for ANNs in the literature [16]. ANN is an efficient tool in pattern recognition. The main advantage of this method is its parallel non-algorithmic distributed architecture for data processing [17]. Because of this advantage, ANN is applied for processing the signals and determination of the fault characteristics.

In this study, a three-layered multiplier perceptron available in MATLAB Neural Network Toolbox is used as an ANN. The algorithm applied for ANN training is Levenberg-Marquardt (LM) feed forward back propagation algorithm. In different fault diagnosis studies, MLP networks with back-propagation algorithms have resulted successfully [16].

A good performance of ANN is achieved through trial and error. In this study, the inputs of the ANN are different features and the outputs are mechanical defect specifications, i.e., mechanical defect type and AD height or RD location. After different tests, the number of layers and the number of neurons in each layer are determined. The final ANN topology has 13 input features, one hidden layer with 10 neurons and 2 outputs. 70% of the dataset is used for training the ANN, i.e., 28 feature sets of RD defects and 11 feature sets of AD defects. The proposed structure for ANN is depicted in Fig. 9.

The obtained signals from different fault conditions are first analyzed for feature selection. The selected features are then inserted to the trained ANN. The output of the trained ANN detects the type, i.e., AD or RD and extent or location of the defect.

The results of the proposed method for RD and AD are shown in TABLE I and TABLE II, respectively. It is clear that the proposed method can detect AD from RD, precisely and no mistake will be made. As shown in TABLE I, all the four degrees of RD are considered as one class for each three double-discs and the proposed method should be able to detect the defect location along the winding correctly for each of these four signals.

The obtained results in TABLE I show that the proposed method can detect the RD along the winding correctly in 29 cases out of 40 total cases, i.e., 72.5% of the cases. Of course, in most cases, the error is just for one consecutive class. As shown in TABLE II, for AD defects, the number of classes is chosen equal to eight, i.e., each two consecutive test cases are assumed as one class. The obtained results show that, through this method, it is possible to detect 13 cases correctly out of 16 total cases. This means that the proposed method can detect AD defects accurately with the rate of 81.25%.

Finally, it should be mentioned that if all the cases are considered simultaneously, this method is able to discriminate between AD and RD accurately without any errors while the accuracy rate of the method for detection of extent and location of AD and RD defects reaches totally to 75%.

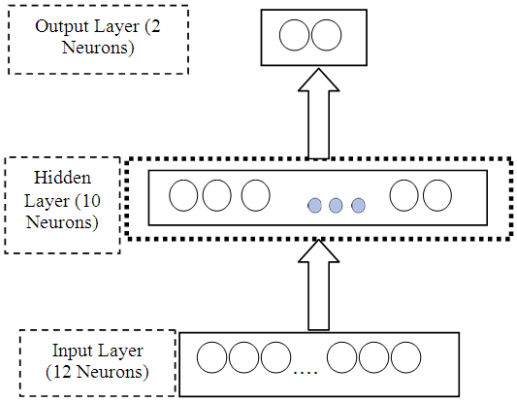

Fig.9. The proposed structure of ANN

TABLE I: The results of the proposed method for radial displacement defect

3-Double-disc No.	Degree No.	RD defect detection	Double-disc No. detection
1	1	√	√
1	2	√	√
1	3	√	√
1	4	√	-
2	1	√	√
2	2	√	√
2	3	√	√
2	4	√	-
3	1	√	√
3	2	√	√
3	3	√	√
3	4	√	√
4	1	√	√
4	2	√	√
4	3	√	-
4	4	√	-
5	1	√	√
5	2	√	-
5	3	√	√
5	4	√	√
6	1	√	-
6	2	√	-
6	3	√	√
6	4	√	√
7	1	√	-
7	2	√	√
7	3	√	-
7	4	√	√
8	1	√	√
8	2	√	√
8	3	√	√
8	4	√	√
9	1	√	√
9	2	√	√
9	3	√	√
9	4	√	√
10	1	√	√
10	2	√	√
10	3	√	-
10	4	√	-

TABLE II: The results of the proposed method for axial displacement defect

Axial displacement amount (cm)	Class number	AD defect detection	Class number detection
0.5	1	√	√
1.0	1	√	√
1.5	2	√	√
2.0	2	√	√
2.5	3	√	√
3.0	3	√	-
3.5	4	√	√
4.0	4	√	√
4.5	5	√	√
5.0	5	√	-
5.5	6	√	√
6.0	6	√	√
6.5	7	√	-
7.0	7	√	√
7.5	8	√	√
8.0	8	√	√

Through comparison of the results obtained for AD and RD, it can be concluded that the identification accuracy rate of RD defects is less than the one obtained for AD. The reason for this fact is related to the characteristics of the presented features for RD. The best characteristic of the feature for the classifier is the linear form, which is not obtained in this study for any type of defects. While most of the features have an injective form for AD, some features do not show a clear pattern for RD. Hence, the ANN classifier is not able to determine the RD location as precise as AD.

In the present work, a method is presented to discriminate and locate two important types of mechanical defects, i.e., RD and AD. This simultaneous detection and location is the most important innovation of the work. For instance, in [19], a method is presented just to classify different faults and locating is not under consideration. Furthermore, in the method presented in [6], it is not possible to locate the mechanical defect as precise as this method.

VI. Conclusion

In this paper, axial displacement and radial deformation as two types of mechanical defects have been investigated and detected through a new method. In the first step, a real transformer has been modeled based on detailed model. Thereafter, these defects in different locations and extends were simulated and a dataset was obtained. In the next step, i.e., feature selection, thirteen features are inserted to the signals. These feature sets are then used in the regression stage. In this stage, the thirteen selected features have been used to train a three-layered multiplier perceptron ANN. The obtained results show that the proposed method can discriminate between axial displacement and radial deformation, completely. Furthermore, it can detect the radial deformation location along the winding or axial displacement extent with a good accuracy.

REFERENCES

[1] T. Y. Ji, W. H. Tang; Q. H. Wu, "Detection of power transformer winding deformation and variation of measurement connections using a hybrid winding model", *Electr. Power Syst. Res.*, vol. 87, 2012, pp. 39-46.

[2] S.A. Ryder, "Diagnosing transformer faults using frequency response analysis", *IEEE Electr. Insul. Mag.*, vol. 19, 2003, pp. 16–22.

[3] L. Satish, S.K. Sahoo, "Locating faults in a transformer winding: an experimental study", *Electr. Power Syst. Res.*, vol. 79, 2009, pp. 89–97.

[4] E. Rahimpour, M. Jabbari and S. Tenbohlen, "Mathematical Comparison Methods to Assess Transfer Functions of Transformers to Detect Different Types of Mechanical Faults", *IEEE Trans. on Power Delivery*, vol. 25, no. 4, Oct. 2010, pp. 2544-2555.

[5] P. Karmifard, G. B. Gharehpetian, "A new algorithm for localization of radial deformation and determination of deformation extent in transformer windings", *Electr. Power Syst. Res.*, vol. 78, 2008, pp. 1701-1711.

[6] P. Karimifard, G. B. Gharehpetian, and S. Tenbohlen, "Localization of winding radial deformation and determination of deformation extent using vector fitting-based estimated transfer function", *Eur. Trans. Elect. Power*, vol. 19, no. 5, Jul., 2009, pp. 749–762.

[7] A. Gray, "Absolute measurements in Electricity and Magnetism", New York: Dover, 1967, pp. 10-20.

[8] A. Miki, T. Hosoya and K. Okuyama, "A calculation method for impulse voltage distribution and transferred voltage in transformer windings", *IEEE Trans. Power Apparat. Syst.*, vol. PAS-97, May/June, 1978, pp. 930-939.

[9] C. Ambrozie, "Teilkapazitaten und grundlegende kapazitanten in scheibenspulentransformatorwicklungen", E & M, Bd. 89, Jahrgang 1972, Heft 9, S. 370-377.

[10] E. Bjerkan, "high frequency modeling of power transofrmers", PhD Dessetation, Trondheim university, 2005.

[11] G. B. Gharehpetian, "Modeling von transformatorwicklungen zue untersuchung schnellveranderlicher transienter vorgange", PhD Dissertation, RWTH Aachen und universitat Tehran, 1996.

[12] E. Rahimpour, J. Christian, K. Feser, H. Mohseni, "Transfer function method to diagnose axial displacement and radial deformation of transformer windings", *IEEE Trans. Power Del.*, vol. 18, no. 2, Apr., pp. 493-505, 2003.

[13] S. Chandaka, A. Chatterjee, S. Munshi, "Cross-correlation aided support vector machine classifier for classification of EEG signals", *Expert Systems with Application*, vol. 36, 2009, pp. 1329-1336.

[14] S. Chandaka, A. Chatterjee and S. Munshi, "Support vector machine employing cross-correlation for emotional speech recognition", Measurement, vol. 42, 2009, pp. 622-618.

[15] K. Pourhossein, G. B. Gharehpetian, E. Rahimpour, B. N. Arabi, " A probabilistic feature to determine type and extent of winding mechanical defects in power transformrs", *Electr. Power Syst. Res.*, vol. 82, 2012, pp. 1-10.

[16] M. A. Hejazi, H. A. Alehosseini and G. B. Gharehpetian, "Detection of transformer winding axial displacement using scattering parameter and ANN", *IEEE Int. Conf. on Power and Energy*, Nov., 2010, pp. 336-340.

[17] A. F. Sultan, G. W. Swift, and D. J. Fedirchuk , "Detection of high impedance arcing faults using a multi-layer perceptron," *IEEE Trans. on Power Delivery*, vol. 7, no. 4, 1992, pp. 1871-1877.

[18] P. V. Goode and M.Y. Chow, "Using a neural/fuzzy system to extract heuristic knowledge of incipient faults in induction motors: Part II-application," *IEEE Trans. Ind. Elect.*, vol. 42, no. 2, pp. 139-146, Apr.1995.

[19] M. Bigdeli, M. Vakilian, and E. Rahimpour, "Transformer winding faults classification based on transfer function analysis by support vector machine", *IET Electr. Power. Appl.*, vol. 6, iss. 5, Aug., 2012, pp. 268-276.

AUTHOR'S PROFILE

Matin Rahmatian

obtained his B.Sc degree in Electrical Engineering from Ferdowsi university of Mashhad, Iran in 2010. Currently, he is an M.Sc student in Electrical Engineering at Amirkabir University of Technology, Tehran, Iran. His research interests include power system and power transformer transients, HVDC transmission systems and micro-grids.

Mehdi S. Naderi

was born in Tabriz, in 1976. He received his BS degree in electrical engineering in 1998 from Sharif University of Technology (SUT), Tehran, Iran and MS and Ph.D. degrees in electrical engineering in 2001 and 2007, respectively from Amirkabir University of Technology (AUT), Tehran, Iran. As a Ph.D. student, he has received scholarship from Iran Power Generation, Transmission and Distribution Management Co. (Tavanir) from May 2005 to Sep 2006 and he has with School of electrical engineering and Telecommunication of the University of New South Wales (UNSW), Sydney, Australia. He has holding the Assistant Professor position in Amirkabir University of Technology (AUT) at Iran Grid Secure Operation Research Center (IGSORC), since 2008.
Dr. Naderi is a member of IAEEE (Iranian Association of Electrical and Electronics Engineers) and Engineers Australia. His teaching and research interests include network planning, power system and transformers transients, FACTS devices, DG and HVDC transmission systems.

G. B. Gharehpetian

received his BS, MS and Ph.D. degrees in electrical engineering in 1987, 1989 and 1996 from Tabriz University, Tabriz, Iran and Amirkabir University of Technology (AUT), Tehran, Iran and Tehran University, Tehran, Iran, respectively, graduating all with First Class Honors. As a Ph.D. student, he has received scholarship from DAAD (German Academic Exchange Service) from 1993 to 1996 and he was with High Voltage Institute of RWTH Aachen, Aachen, Germany.
He has been holding the Assistant Professor position at AUT from 1997 to 2003, the position of Associate Professor from 2004 to 2007 and has been Professor since 2007. He was selected by the ministry of higher education as the distinguished professor of Iran and by IAEEE (Iranian Association of Electrical and Electronics Engineers) as the distinguished researcher of Iran and was awarded the National Prize in 2008 and 2010, respectively.
He is the author of more than 650 journal and conference papers. His teaching and research interest include power system and transformers transients and power electronics applications in power systems.

A. J. Ghanizadeh

was born in Herat, Afghanistan, in 1981. He received his B.Sc. and M.Sc. in electrical engineering from Sahand University of Technology, Tabriz, Iran and Ferdowsi University of Mashhad, Mashhad, Iran, in 2004 and 2009, respectively. He is currently pursuing the Ph.D. degree in the electrical engineering department at the Amirkabir University of Technology (AUT), Tehran, Iran. His research interests include Power Quality, power system optimization and operation and transformers transients.